Springer Series in Materials Science 215

Carlo Massobrio
Jincheng Du
Marco Bernasconi
Philip S. Salmon *Editors*

Molecular Dynamics Simulations of Disordered Materials

From Network Glasses to Phase-Change Memory Alloys

Springer

Springer Series in Materials Science

Volume 215

The Springer Series in Materials Science covers the complete spectrum of materials physics, including fundamental principles, physical properties, materials theory and design. Recognizing the increasing importance of materials science in future device technologies, the book titles in this series reflect the state-of-the-art in understanding and controlling the structure and properties of all important classes of materials.

More information about this series athttp://www.springer.com/series/856

Carlo Massobrio · Jincheng Du
Marco Bernasconi · Philip S. Salmon
Editors

Molecular Dynamics Simulations of Disordered Materials

From Network Glasses to Phase-Change Memory Alloys

Springer

Editors
Carlo Massobrio
IPCMS
Strasbourg University
Strasbourg
France

Marco Bernasconi
Department of Materials Science
University of Milan Bicocca
Milan
Italy

Jincheng Du
Department of Materials Science
and Engineering
University of North Texas
Denton, TX
USA

Philip S. Salmon
Department of Physics
University of Bath
Bath
UK

ISSN 0933-033X ISSN 2196-2812 (electronic)
Springer Series in Materials Science
ISBN 978-3-319-15674-3 ISBN 978-3-319-15675-0 (eBook)
DOI 10.1007/978-3-319-15675-0

Library of Congress Control Number: 2015933149

Springer Cham Heidelberg New York Dordrecht London

Printed on acid-free paper

Springer International Publishing AG Switzerland is part of Springer Science+Business Media (www.springer.com)

Preface

The purpose of this book is to identify current achievements and properly assess the state of the art in the atomic scale modelling of structurally disordered (glassy) materials. More precisely, we intend to bring to the attention of the readership representative examples of systems for which the structural information provided by molecular dynamics has been instrumental in bringing significant progresses in the area of glass science. The underlying motivation of this collection of contributions rests on the notion that glassy materials are intrinsically devoid of regular structural organization.

Early attempts to extract information on glass structure were based on a combination of indirect experimental evidence (quite often obtained by associating measured spectral features with specific crystalline-like motifs) and phenomenological models. The resulting descriptions of the glass structures were highly qualitative and unable to account for the role of chemical bonding in determining the nature of the structural units, their connectivity as well as the extent of their correlation and order. Advances in algorithms and high performing computer facilities capable of handling realistic models and to extend the size and timescale of dynamical simulations have represented a major step forward in promoting this class of simulations to reliable *virtual* experiments. Indeed, recent years have witnessed the advent of atomic scale modelling as a new approach for understanding the properties of glass. This approach is characterized by a clear distinction between the notion of "glasses" as ideal "statistical mechanics" models and their treatment as real materials of interest in material science and technology. By focusing on real glasses a computational material scientist seeks a precise knowledge of structural properties for a given system by using quantitative tools. This strategy is radically different from qualitative assessments that are equally valid and applicable to any disordered system but do not target any correlation between atomic structure and bonding properties. Investigating glasses in the framework of computational material science is a theoretical strategy legitimated by the increased

reliability of both classical molecular dynamics (CMD) and first-principles molecular dynamics (FPMD). This will be exemplified in this book and it is fully substantiated by the observation that CMD and FPMD are able to produce models more and more realistic, since their predictive power increases at a very fast pace.

To set the scene for a proper account of relevant issues in the area of disordered network, this volume opens with a contribution (by Philip S. Salmon and Anita Zeidler) having a predominant experimental character and yet containing several useful considerations on the role played by atomic scale modelling in the understanding of short and intermediate range order. While the essence of classical molecular dynamics is intuitively accessible to any practitioner willing to model a system by employing a suitable interatomic potential, the concepts inherent in first-principles molecular dynamics are less straightforward to grasp. This is because FPMD requires the knowledge and the control of a specific methodology combining electronic structure concepts and newtonian dynamics. For this reason, a chapter written by Mauro Boero and co. is devoted to this issue. Moving a further step into the methodology to tackle problems related to the glassy state organization, the contribution by the team of Riccardo Mazzarello focuses on metadynamics as a tool to understand nucleation and phase changes involving the disordered state. Moving into actual modelling of glassy materials, the proper description of iono-covalent bonding is extremely challenging within an effective interatomic potential framework. In the first contribution devoted to modelling of glasses within classical (and yet realistic) molecular dynamics, Liping Huang and John Kieffer are able to describe under which conditions potential models can be used to study archetypical, iono-covalent glass formers. Along the same lines, Pedone and Menziani address the issue of the development of reliable and transferable empirical potentials, optimization of the glass forming procedures and experimental validation of the resulting structures. At the crossroad between simulation methodology (applied to amorphous recrystallization) and realistic modelling of interface phenomena, the classical modelling developed by Evelyne Lampin is able to account for the morphology and the dynamics of a crystal/amorphous interface. In his contribution, Jincheng Du addresses the issue of atomic-scale modelling of multicomponent oxide glasses. Once again, the focus is on the capabilities of classical molecular dynamics to model (with no explicit account of the electronic structure) interactions requiring the account of polarizability for systems that can contain several hundred thousand atoms. The team of Monia Montorsi is also very much concerned by this issue, as shown by the quite realistic modelling of complex transition metal oxides. The section of the book devoted to the applications of classical molecular dynamics models and methods ends with a large series of examples (by Mark Wilson) for silica and carbon system, based on highly refined interatomic potentials containing n-body and/or polarization effects. Interestingly, these models turn out to be quite realistic for systems having different dimensionalities. At the crossroad between classical and first-principles molecular dynamics, Antonio Tilocca addresses a very

important issue of glass science, namely the role of these materials in determining and regulating biological functions such as biodegradation. Dynamical effects are nicely highlighted, within the framework of surface reactivity and ion migration. First-principles molecular dynamics (FPMD) is the common ingredient of the last set of contributions, all inspired and nurtured by the predictive power of electronic structure calculations for the potential energy surfaces, combined with newtonian dynamics. For instance, Matthieu Micoulaut establishes the link between the connectivity of such realistic models and the topological constraint theory. The contribution by Assil Bouzid and co. (C. Massobrio/M. Boero team) traces back the modelling of Ge_xSe_{1-x} chalcogenides from the early stages until the last realizations, with a focus on the comparison between $GeSe_4$ and GeS_4 glasses. The peculiar properties of glass surfaces (for silica and chalcogenides) are addressed by Guido Ori and co., with implications for the development of classic force fields based on a consistent definition of charges depending on the local environment. The case of a prototypical network-forming systems based on trigonal units is presented in great detail by Guillaume Ferlat, focussing on the ring structure of glassy B_2O_3. First-principles molecular dynamics approaches have been widely employed in recent years to gain valuable insight into the properties of a very important class of disordered networks, the so-called phase change materials. These are of great interest for optical recording and memory devices. This books ends with five contributions related to the structural and bonding properties of specific chalcogenide alloys very much employed in this context. As shown by Caravati and co., FPMD can also be used as an input for the creation of smart interatomic potentials (the so-called Neural Network ones) enabling realistic crystallization studies on quite large samples (4000 atoms). Structure and crystallization dynamics are also tackled by Jaakko Akola and co. on the prototypical phase change material (PCM hereafter and in the remainder of the book) $Ge_2Sb_2Te_5$, while a large variety of structural behaviours common to sub-systems inherent in the PCMs are reviewed in the contribution by Jean-Yves Raty and co., with a special emphasis for the criterion of structural stability. Finally, the effect of doping on phase change materials is considered in the contribution of the teams headed by David Drabold and Stephen Elliott, respectively. While both contain information on transition metal doping, the second paper also provides information on carbon and nitrogen doping.

Overall, we are convinced that the research efforts presented in this volume are higly representative of the impact of atomic-scale molecular dynamics modelling towards the understanding of structural and topological features of glass. Whenever it appears possible, sufficiently realistic and convenient, glass can be simulated by using interatomic potential, these tools becoming more and more refined, especially when they are derived from electronic structure potential energy surfaces. For situations where the accuracy of first-principle molecular dynamics is required, glasses are studied via a quantitative account of chemical bonding, through

first-principles molecular dynamics, yielding trajectories that evolve self-consistently as a function of the network topology and of the changes induced by temperature.

Based on the above assertions, we conclude that molecular dynamics applied to glass has evolved from a computer-based tool complementary to experiments to a reliable and authoritative source of atomic-scale information on its own.

Strasbourg

Carlo Massobrio
Jincheng Du
Marco Bernasconi
Philip S. Salmon

Contents

Contributors

Jaakko Akola Department of Physics, Tampere University of Technology, Tampere, Finland

M. Bauchy Department of Civil and Environmental Engineering, University of California, Los Angeles, CA, USA

Marco Bernasconi Department of Materials Science, University of Milano-Bicocca, Milano, Italy

Christophe Bichara CINAM—CNRS Université Aix-Marseille, Marseille Cedex 9, France

Mauro Boero Institut de Physique et Chimie des Materiaux de Strasbourg (IPCMS), University of Strasbourg—CNRS UMR 7504, Strasbourg, France

Assil Bouzid Institut de Physique et Chimie des Materiaux de Strasbourg (IPCMS), University of Strasbourg—CNRS UMR 7504, Strasbourg, France

Giulia Broglia Department of Science and Methods for Engineering, University of Modena and Reggio Emilia, Reggio Emilia, Italy

Sebastiano Caravati Department of Materials Science, University of Milano-Bicocca, Milano, Italy

B. Coasne Multiscale Materials Science for Energy and Environment, CNRS-MIT (UMI 3466), Cambridge, MA, USA; Institut Charles Gerhard Montpellier, CNRS (UMR 5253), ENSCM, Université Montpellier 2, Montpellier Cedex 5, France; Department of Civil and Environmental Engineering, Massachusetts Institute of Technology, Cambridge, MA, USA

D.A. Drabold Department of Physics and Astronomy, Ohio University, Athens, Ohio, USA

Jincheng Du Department of Materials Science and Engineering, University of North Texas, Denton, TX, USA

S.R. Elliott Department of Chemistry, University of Cambridge, Bath, UK

Guillaume Ferlat IMPMC, Université Pierre et Marie Curie, Paris, France

H. Flores-Ruiz Laboratoire de Physique Thorique de la Matire Condense, Paris Cedex 05, France

Liping Huang Department of Materials Science and Engineering, Rensselaer Polytechnic Institute, Troy, NY, USA

Robert O. Jones Peter Grünberg Institut PGI-1 and JARA/HPC, Forschungszentrum Jülich, Jülich, Germany

Janne Kalikka Singapore University of Technology and Design, Singapore, Singapore

John Kieffer Department of Materials Science and Engineering, University of Michigan, Ann Arbor, MI, USA

Evelyne Lampin Institute of Electronics, Microelectronics and Nanotechnology, Villeneuve d'Ascq Cedex, France

Sébastien Le Roux Institut de Physique et Chimie des Materiaux de Strasbourg (IPCMS), University of Strasbourg—CNRS UMR 7504, Strasbourg, France

T.H. Lee Department of Chemistry, University of Cambridge, Bath, UK

Vincenzo Lordi Lawrence Livermore National Laboratory, Livermore, CA, USA

Carlo Massobrio Institut de Physique et Chimie des Materiaux de Strasbourg (IPCMS), University of Strasbourg—CNRS UMR 7504, Strasbourg, France

Riccardo Mazzarello Institute for Theoretical Solid State Physics, RWTH Aachen, Aachen, Germany

Maria Cristina Menziani Dipartimento di Scienze Chimiche e Geologiche, Università degli Studi di Modena e Reggio Emilia, Modena, Italy

M. Micoulaut Laboratoire de Physique Thorique de la Matire Condense, Paris Cedex 05, France

Monia Montorsi Department of Science and Methods for Engineering, University of Modena and Reggio Emilia, Reggio Emilia, Italy

Consuelo Mugoni Department of Engineering "Enzo Ferrari", University of Modena and Reggio Emilia, Modena, Italy

Guido Ori Multiscale Materials Science for Energy and Environment, CNRS-MIT (UMI 3466), Cambridge, MA, USA; Institut Charles Gerhardt Montpellier, CNRS UMR 5253, University of Montpellier II, ENSCM, Montpellier, France; Institut de Physique et Chimie des Matériaux de Strasbourg, University of Strasbourg—CNRS UMR 7504, Strasbourg, France

Céline Otjacques Physics of Solids, Interfaces and Nanostructures, University of Liége B5, Liége, Belgium

Burak Ozdamar Institut de Physique et Chimie des Materiaux de Strasbourg (IPCMS), University of Strasbourg—CNRS UMR 7504, Strasbourg, France

Alfonso Pedone Dipartimento di Scienze Chimiche e Geologiche, Università degli Studi di Modena e Reggio Emilia, Modena, Italy

Rengin Peköz Max Planck Institute for Polymer Research, Mainz, Germany

Binay Prasai Department of Physics and Astronomy, Ohio University, Athens, Ohio, USA

Jean-Yves Raty Physics of Solids, Interfaces and Nanostructures, University of Liége B5, Liége, Belgium

Ider Ronneberger Institute for Theoretical Solid State Physics, RWTH Aachen, Aachen, Germany

Philip S. Salmon Department of Physics, University of Bath, Bath, UK

J.M. Skelton Department of Chemistry, University of Bath, Bath, UK

Gabriele C. Sosso Faculty of Maths and Physical Sciences, London Centre for Nanotechnology, University College London, London, UK

Antonio Tilocca Department of Chemistry, University College London, London, UK

Christine Tugène Institut de Physique et Chimie des Matériaux de Strasbourg, University of Strasbourg—CNRS UMR 7504, Strasbourg, France

Mark Wilson Physical and Theoretical Chemistry Laboratory, Department of Chemistry, University of Oxford, Oxford, UK

Anita Zeidler Department of Physics, University of Bath, Bath, UK

Chapter 1
The Atomic-Scale Structure of Network Glass-Forming Materials

Philip S. Salmon and Anita Zeidler

Abstract A prerequisite for understanding the physico-chemical properties of network glass-forming materials is knowledge about their atomic-scale structure. The desired information is not, however, easy to obtain because structural disorder in a liquid or glass leads to complexity. It is therefore important to design experiments to give site-specific information on the structure of a given material in order to test the validity of different molecular dynamics models. In turn, once a molecular dynamics scheme contains the correct theoretical ingredients, it can be used both to enrich the information obtained from experiment and to predict the composition and temperature/pressure dependence of a material's properties, a first step in using the principles of rational design to prepare glasses with novel functional properties. In this chapter the symbiotic relationship between experiment and simulation is explored by focussing on the structures of liquid and glassy $ZnCl_2$ and $GeSe_2$, and on the structure of glassy GeO_2 under pressure. Issues to be addressed include extended range ordering on a nanometre scale, the formation of homopolar (like-atom) bonds, and the density-driven mechanisms of network collapse.

1.1 Introduction

Network glass-forming materials are important in a broad range of scientific and technological disciplines, ranging from photonics [1] to magmas in planetary science [2]. It is therefore desirable to have realistic microscopic models of these materials in order to predict their behaviour when different chemical components are added, and when the state conditions are changed. A prerequisite for guiding in the development of a model is unambiguous information from experiment on the atomic-scale structure and dynamics in order to provide a critical test of its predictions.

P.S. Salmon (✉) · A. Zeidler
Department of Physics, University of Bath, Bath BA2 7AY, UK
e-mail: p.s.salmon@bath.ac.uk

A. Zeidler
e-mail: a.zeidler@bath.ac.uk

C. Massobrio et al. (eds.), *Molecular Dynamics Simulations of Disordered Materials*, Springer Series in Materials Science 215,
DOI 10.1007/978-3-319-15675-0_1

Structure refinement methods such as Reverse Monte Carlo (RMC) [3, 4] and Empirical Potential Structure Refinement (EPSR) [5, 6] are widely used by experimentalists to model measured diffraction data. In these methods, the atoms in a 3-dimensional starting model are moved in order to give configurations with diffraction patterns that are in agreement with experiment, subject to imposed constraints such as the measured number density, the inability of neighbouring particles to overlap, and the type and quantity of local structural units as provided by e.g. nuclear magnetic resonance (NMR) and/or extended x-ray absorption fine structure (EXAFS) spectroscopy experiments. The structural models therefore have the benefit of being consistent with the experimental data used in their construction[1] and, since they are based on 3-dimensional particle configurations, information can be obtained on three- and higher-body correlations. The reliability of the structural features in a given model will, however, depend on the sensitivity of the experimental data to the relevant correlations, the results for higher body correlations need to be treated with caution because diffraction data provides information only at the pair-correlation function level, and the final configurations can be sensitive to the choice of starting model as shown by work on SiO_2 glass [7, 8] and water [9–11]. For this reason, it is usually best to construct a realistic starting model so that the use of RMC or EPSR amounts to a refinement of that model using the experimental results as a reference.[2] Owing to the nature of their construction, RMC or EPSR models do not provide information on the particle dynamics, and since the modelling procedures are driven by experimental data they cannot be used if this information is unavailable i.e. the refinement methods have in this sense no predictive power.

Molecular dynamics methods, which are extensively used to model the structure of network glass-forming materials, also provide the atomic-scale dynamics (e.g. the vibrational density of states and self-diffusion coefficients), thus enriching the information made available on a given material. A comparison of this dynamical information with experiment can provide a particularly severe test for the validity of a model for a particular material. Furthermore, if the theory underlying the calculations has the correct ingredients then the simulations can be used to predict the composition and temperature/pressure dependence of a material's properties. Oftentimes, the search for the correct theoretical ingredients is not, however, trivial and different approaches involve trade-offs between e.g. the accuracy in describing a particular bonding scheme versus the number of atoms that can be dealt with on a realistic computational timescale.

For example, ionic interaction models can give an accurate description of the measured structure of glass-forming systems such as $ZnCl_2$ [14–17], provided that anion polarisation effects are taken into account [18–20], and the relative simplicity of these models allows for the coverage of relatively long length and time scales. Such models are, however, inappropriate for glass-forming materials such as $GeSe_2$ where

[1] In the literature, the results from RMC or EPSR models are sometimes erroneously referred to as 'experimental results' when comparisons are made with molecular dynamics simulations.

[2] Increasingly, molecular dynamics is being used to provide the starting models for refinement procedures, see e.g. [12, 13].

the electronegativity difference between the atomic species is small and homopolar (like-atom) bonds are prevalent [21–23]. These features necessitate a first-principles density-functional based approach in which the electronic structure is taken into explicit account but where the simulation results can be sensitive to the choice of density functional [24–40]. These methods allow only for the investigation of relatively small systems for short times, although this may not be such an important issue when investigating e.g. the operation of phase-change memory alloys where the pertinent length and time scales are small relative to those associated with glass formation. In the investigation of glass-forming materials, there is also the question as how best to prepare accurate molecular dynamics models given the use of fast simulated quench-rates [37, 41–43].

In the following, the role of experiment in guiding molecular dynamics simulations of network glass-forming systems will be illustrated by considering a small set of materials with the MX_2 stoichiometry. Particular attention will be paid to the results obtained from the method of neutron diffraction with isotope substitution (NDIS) since it has been extensively used to obtain information at the partial structure factor level. An excellent starting point is provided by molten MX_2 salts where NDIS results have helped in the development of a reliable ionic interaction model for glass-forming materials like $ZnCl_2$. Next, the $GeSe_2$ system is considered where NDIS results have played a major role in the continuing development of first-principles molecular dynamics methods for describing the structure and properties of this and other chalcogenide glass-formers.[3] Finally, GeO_2 glass is considered where the results from recent in situ high-pressure NDIS experiments are helping to arbitrate between competing molecular dynamics models for the density-driven network collapse.

1.2 Outline Diffraction Theory

In a neutron diffraction experiment on a liquid or glassy MX_2 system, the coherent scattered intensity measured with respect to the magnitude of the scattering vector k can be represented by the total structure factor [44]

$$F(k) = c_{\mathrm{M}}^2 b_{\mathrm{M}}^2 [S_{\mathrm{MM}}(k) - 1] + 2c_{\mathrm{M}} c_{\mathrm{X}} b_{\mathrm{M}} b_{\mathrm{X}} [S_{\mathrm{MX}}(k) - 1] + c_{\mathrm{X}}^2 b_{\mathrm{X}}^2 [S_{\mathrm{XX}}(k) - 1] \qquad (1.1)$$

where c_α and b_α denote the atomic fraction and bound coherent scattering length of chemical species α, respectively. $S_{\alpha\beta}(k)$ is a so-called Faber-Ziman [45] partial structure factor which is related to the partial pair-distribution function $g_{\alpha\beta}(r)$ by the Fourier transform relation

[3] Chalcogenide glass-forming materials are those containing one or more of the chalcogen elements S, Se and Te.

$$g_{\alpha\beta}(r) = 1 + \frac{1}{2\pi^2 \rho\, r} \int_0^\infty \mathrm{d}k\, k \left[S_{\alpha\beta}(k) - 1\right] \sin(kr), \tag{1.2}$$

where ρ is the atomic number density of the system and r is a distance in real space. The mean coordination number of atoms of type β, contained in a volume defined by two concentric spheres of radii r_1 and r_2 centred on an atom of type α, is given by

$$\bar{n}_\alpha^\beta = 4\pi\, \rho\, c_\beta \int_{r_1}^{r_2} \mathrm{d}r\, r^2 g_{\alpha\beta}(r). \tag{1.3}$$

The full set of $S_{\alpha\beta}(k)$ functions for an MX_2 system can be extracted from the measured diffraction patterns by applying the NDIS method, provided that isotopes are available with a sufficiently large neutron scattering length contrast [44, 46, 47].

The total structure factor can also be expressed in terms of the Bhatia-Thornton [48] number-number, concentration-concentration and number-concentration partial structure factors denoted by $S_{\mathrm{NN}}(k)$, $S_{\mathrm{CC}}(k)$ and $S_{\mathrm{NC}}(k)$, respectively. These partial structure factors are related to fluctuations (in the liquid or glass) of the number density, concentration and their cross-correlation, respectively. Equation (1.1) can be re-written as

$$\begin{aligned} F(k) = {} & \langle b \rangle^2 \left[S_{\mathrm{NN}}(k) - 1\right] + c_{\mathrm{M}} c_{\mathrm{X}} (b_{\mathrm{M}} - b_{\mathrm{X}})^2 \left\{\left[S_{\mathrm{CC}}(k)/c_{\mathrm{M}} c_{\mathrm{X}}\right] - 1\right\} \\ & + 2 \langle b \rangle (b_{\mathrm{M}} - b_{\mathrm{X}}) S_{\mathrm{NC}}(k) \end{aligned} \tag{1.4}$$

where $\langle b \rangle = c_{\mathrm{M}} b_{\mathrm{M}} + c_{\mathrm{X}} b_{\mathrm{X}}$ is the average coherent neutron scattering length. The relationships between the two sets of partial structure factors are given by

$$S_{\mathrm{NN}}(k) = c_{\mathrm{M}}^2 S_{\mathrm{MM}}(k) + c_{\mathrm{X}}^2 S_{\mathrm{XX}}(k) + 2 c_{\mathrm{M}} c_{\mathrm{X}} S_{\mathrm{MX}}(k), \tag{1.5}$$

$$S_{\mathrm{CC}}(k) = c_{\mathrm{M}} c_{\mathrm{X}} \left\{1 + c_{\mathrm{M}} c_{\mathrm{X}} \left[S_{\mathrm{MM}}(k) + S_{\mathrm{XX}}(k) - 2 S_{\mathrm{MX}}(k)\right]\right\}, \tag{1.6}$$

$$S_{\mathrm{NC}}(k) = c_{\mathrm{M}} c_{\mathrm{X}} \left\{c_{\mathrm{M}} \left[S_{\mathrm{MM}}(k) - S_{\mathrm{MX}}(k)\right] - c_{\mathrm{X}} \left[S_{\mathrm{XX}}(k) - S_{\mathrm{MX}}(k)\right]\right\}. \tag{1.7}$$

The Fourier transforms of $S_{\mathrm{NN}}(k)$, $S_{\mathrm{CC}}(k)$ and $S_{\mathrm{NC}}(k)$ are the partial pair-distribution functions $g_{\mathrm{NN}}(r)$, $g_{\mathrm{CC}}(r)$ and $g_{\mathrm{NC}}(r)$, respectively. The relationships between the $g_{IJ}(r)$ (I, J = N, C) and $g_{\alpha\beta}(r)$ (α, β = M, X) functions are given by

$$g_{\mathrm{NN}}(r) = c_{\mathrm{M}}^2 g_{\mathrm{MM}}(r) + c_{\mathrm{X}}^2 g_{\mathrm{XX}}(r) + 2 c_{\mathrm{M}} c_{\mathrm{X}} g_{\mathrm{MX}}(r), \tag{1.8}$$

$$g_{\mathrm{CC}}(r) = c_{\mathrm{M}} c_{\mathrm{X}} \left[g_{\mathrm{MM}}(r) + g_{\mathrm{XX}}(r) - 2 g_{\mathrm{MX}}(r)\right], \tag{1.9}$$

$$g_{\mathrm{NC}}(r) = c_{\mathrm{M}} \left[g_{\mathrm{MM}}(r) - g_{\mathrm{MX}}(r)\right] - c_{\mathrm{X}} \left[g_{\mathrm{XX}}(r) - g_{\mathrm{MX}}(r)\right]. \tag{1.10}$$

If $b_{\mathrm{M}} = b_{\mathrm{X}}$ the incident neutrons in a diffraction experiment cannot distinguish between the different scattering nuclei and the measured total structure factor gives $S_{\mathrm{NN}}(k)$ directly (see (1.4)). The corresponding Fourier transform $g_{\mathrm{NN}}(r)$ therefore

describes the sites of the scattering nuclei and, since it cannot distinguish between the chemical species that decorate those sites, it gives information on the topological ordering. If $\langle b \rangle = 0$, however, the measured total structure factor gives $S_{CC}(k)$ directly and its Fourier transform $g_{CC}(r)$ describes the chemical ordering of the M and X atomic species. The $g_{CC}(r)$ function will have a positive or negative peak at a given distance when there is a preference for like or unlike neighbours, respectively (see (1.9)). The $g_{NC}(r)$ function describes the correlation between the sites described by $g_{NN}(r)$ and their occupancy by a given chemical species.

In practice, a diffractometer can only access a finite k-space range with a maximum cutoff value k_{max}. Provided that sufficiently small k-values can be accessed, a reciprocal-space function such as $F(k)$ will therefore be truncated by a modification function given by $M(k) = 1$ for $k \leq k_{max}$ and $M(k) = 0$ for $k > k_{max}$. In consequence, the real-space information corresponding to $F(k)$ is obtained by the Fourier transform relation

$$G(r) = \frac{1}{2\pi^2 \rho r} \int_0^\infty \mathrm{d}k \, k \, F(k) M(k) \sin(kr). \tag{1.11}$$

The desired r-space information is therefore convoluted with the Fourier transform of $M(k)$, the effect of which becomes negligible if k_{max} is sufficiently large that $F(k)$ is featureless at higher k-values. To give smoother r-space functions, other expressions for $M(k)$ are used such as the Lorch [49] modification function where $M(k) = \sin(\pi k/k_{max})/(\pi k/k_{max})$ for $k \leq k_{max}$ and $M(k) = 0$ for $k > k_{max}$.[4] To facilitate a like-for-like comparison between measured and molecular dynamics results, the reciprocal-space functions constructed from simulations are often Fourier transformed according to (1.11) with k_{max} set at the experimental value.

1.3 Ionic Interaction Models for MX_2 Glass-Forming Materials

The NDIS method has been used to measure the full set of partial structure factors for molten salts with the MX_2 stoichiometry. The effect on the structure of varying the cation to anion size ratio was thereby investigated for liquid $BaCl_2$ [51], $SrCl_2$ [52], $CaCl_2$ [53], $MgCl_2$ [54], $NiCl_2$ [55] and $ZnCl_2$ [14] where the radius of Cl^- is 1.81 Å and the cation radii are 1.35 Å (Ba^{2+}), 1.18 Å (Sr^{2+}), 1.00 Å (Ca^{2+}), 0.72 Å (Mg^{2+}), 0.69 Å (Ni^{2+}) and 0.74 Å (Zn^{2+}) [56].[5] Of these liquids, only $ZnCl_2$ readily forms a glass by bulk-quenching methods, and corner-sharing $ZnCl_4$ tetrahedra are the predominant structural motifs.

[4] A rigorous derivation of the Lorch modification function and its corresponding real-space representation is given in [50].

[5] The radii correspond to six-fold coordinated ions.

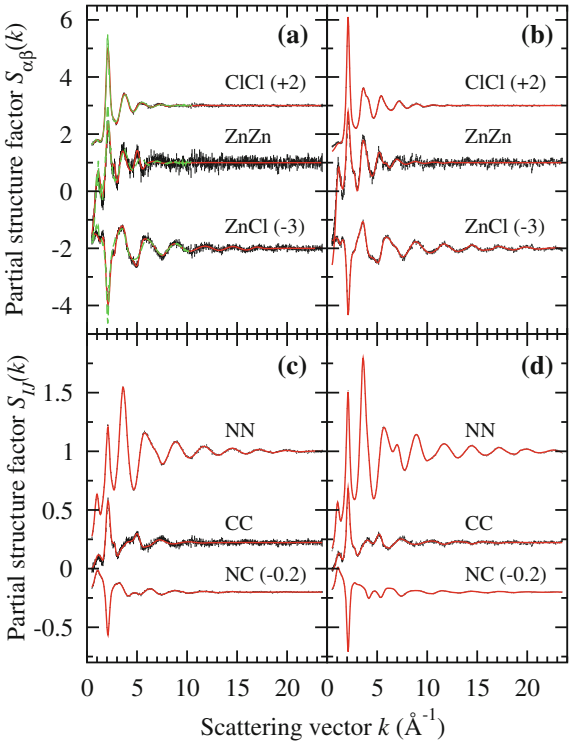

Fig. 1.1 The Faber-Ziman $S_{\alpha\beta}(k)$ (α, β = M, X) and Bhatia-Thornton $S_{IJ}(k)$ (I, J = N, C) partial structure factors for liquid and glassy $ZnCl_2$. The points with vertical (*black*) error bars are the measured functions in (**a**) and (**c**) for the liquid at 332(5) °C [16] and in (**b**) and (**d**) for the glass at 25(1) °C [15, 16]. The solid (*red*) curves are the Fourier back transforms of the corresponding partial pair-distribution functions after the unphysical oscillations at r-values smaller than the distance of closest approach between the centres of two atoms are set to the calculated limit at $r = 0$. The broken (*green*) curves in (**a**) are from the polarisable ion model of Sharma and Wilson [63] for the liquid at 327 °C

The full set of partial structure factors recently measured for liquid and glassy $ZnCl_2$ are shown in Fig. 1.1 [15, 16]. The prominent first sharp diffraction peak (FSDP) in $S_{ZnZn}(k)$ at a scattering vector $k_{FSDP} \simeq 1$ Å^{-1} is a signature of structural complexity on an intermediate length scale with a periodicity given by $2\pi/k_{FSDP}$ and with a correlation length given by $2\pi/\Delta k_{FSDP}$ where Δk_{FSDP} is the full-width at half-maximum of the FSDP [57]. As shown in Fig. 1.1, the principal peaks[6] in the Faber-Ziman partial structure factors align at a common scattering vector $k_{PP} \simeq 2.1$ Å^{-1} and it follows from (1.5)–(1.7) that the principal peaks in the Bhatia-Thornton [48] partial structure factors $S_{IJ}(k)$ also align at this common position. The measured $S_{NN}(k)$ function for the liquid shows a clear 'three-peak' character that is not shared

[6] A so-called principal peak or trough at $k_{PP} \simeq 2$–3 Å^{-1} is a common feature in the partial structure factors for liquid and glassy materials [47].

with the other molten salts listed above, and all of the partial structure factors $S_{IJ}(k)$ (I, J = N, C) for both the liquid and glass display an FSDP [58, 59] e.g. there are concentration fluctuations on an intermediate length scale that will be discussed further in Sect. 1.4.3.

The experimental results for molten $ZnCl_2$ feature a nearest-neighbour Zn–Zn distance that is comparable to the nearest-neighbour Cl–Cl distance. This observation is not expected on the basis of a rigid ion model (RIM) for the interionic interactions in which the ions are non-deformable and the Coulomb repulsion between divalent cations is large. The experimental results for molten $ZnCl_2$ have therefore been attributed to a manifestation of 'covalent' effects in the bonding [60]. As shown by Wilson and Madden [18], however, it is possible to describe the structure of $ZnCl_2$ within the framework of an ionic interaction model, provided that account is taken of the anion polarisability α_X. The effect of this polarisability is shown in Fig. 1.2 where two simulations are made on an MX_2 system in which the M^{2+} and X^- ions take full formal charges but α_X is either set to zero, corresponding to a RIM, or set to 20 au, corresponding to a polarisable ion model (PIM) [61]. An FSDP develops in $S_{MM}(k)$ at $k_{FSDP} \simeq 1.2$ Å^{-1} as the anion polarisability is increased to $\alpha_X = 20$ au and the principal peaks in all three of the Faber-Ziman partial structure factors align at a common value $k_{PP} \simeq 2$ Å^{-1}. The anion polarisation shields the Coulomb repulsion between divalent cations which reduces the mean M-X-M bond angle between MX_4 tetrahedra, leading to a shortening of the mean M-M distance relative to the RIM. This shielding leads to regions in which there is either an enhanced or diminished

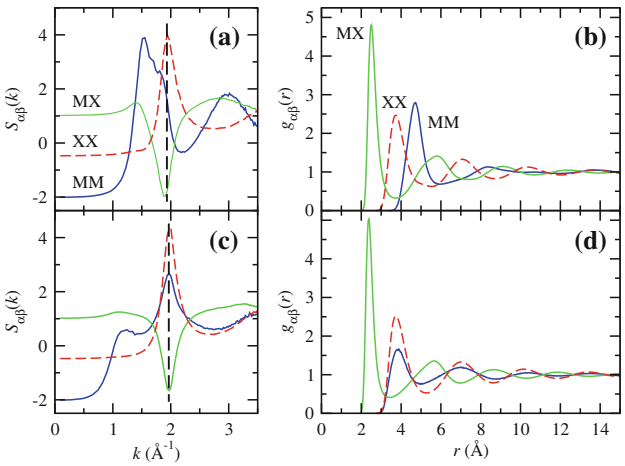

Fig. 1.2 The Faber-Ziman partial structure factors $S_{\alpha\beta}(k)$ and partial pair-distribution functions $g_{\alpha\beta}(r)$ (α, β = M, X) as calculated for models using two different values for the anion polarisability α_X [61]. The curves in (**a**) and (**b**) correspond to a rigid ion model (RIM) with $\alpha_X = 0$, while the curves in (**c**) and (**d**) correspond to a polarisable ion model (PIM) with $\alpha_X = 20$ au. The introduction of anion polarisability leads to the appearance of an FSDP in $S_{MM}(k)$ at $k_{FSDP} \simeq 1.2$ Å^{-1} and to an alignment of the principal peaks in all three $S_{\alpha\beta}(k)$ functions at $k_{PP} \simeq 2$ Å^{-1}. The alignment of the principal peaks in (**c**) arises from in-phase large-r oscillations in the $g_{\alpha\beta}(r)$ functions shown in (**d**)

cation density relative to a RIM [62] i.e. there is a modulation of the cation-cation correlations on an intermediate length scale that gives rise to the FSDP in $S_{\mathrm{MM}}(k)$. The $S_{\alpha\beta}(k)$ functions predicted for liquid $ZnCl_2$ by using a PIM with $\alpha_{\mathrm{X}} = 20$ au [63] are shown in Fig. 1.1a.

On cooling a liquid to form a glass, there is a sharpening of the peaks in the measured partial structure factors in accordance with a loss of thermal disorder (Fig. 1.1). Since the FSDP is already a sharp feature and is the peak that occurs at the smallest k-value, it might be expected to dominate the large-r behaviour of the partial pair-distribution functions. This is not, however, the case as can be shown by investigating the Bhatia-Thornton partial pair-correlation functions $rh_{\mathrm{NN}}(r) \equiv r\,[g_{\mathrm{NN}}(r) - 1]$, $rh_{\mathrm{CC}}(r) \equiv rg_{\mathrm{CC}}(r)$ and $rh_{\mathrm{NC}}(r) \equiv rg_{\mathrm{NC}}(r)$, which enable a separation of the contributions to the structure from topological versus chemical ordering [15, 50, 64, 65]. As shown in Fig. 1.3, the measured $rh_{IJ}(r)$ functions for $ZnCl_2$ glass show

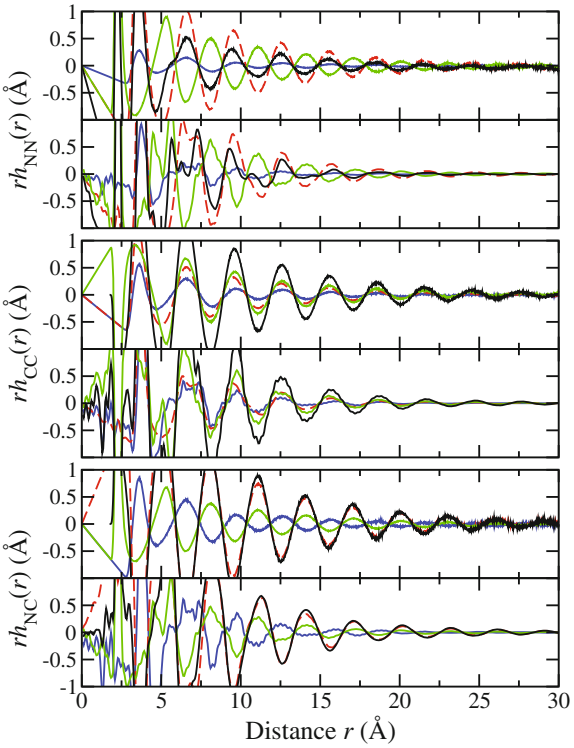

Fig. 1.3 The Bhatia-Thornton pair-correlation functions $rh_{IJ}(r)$ (I, J = N, C) [solid dark (*black*) curves] where the upper, middle and lower pairs of panels show the NN, CC and NC functions, respectively. For each pair, the upper panel gives the function obtained for a polarisable ion model (PIM) with $\alpha_{\mathrm{X}} = 20$ au [20] and the lower panel gives the measured function for glassy $ZnCl_2$ [15, 16]. Each function is broken down into its contributions from $rh_{\mathrm{XX}}(r)$ [broken (*red*) curves], $rh_{\mathrm{MX}}(r)$ [light solid (*green*) curves] and $rh_{\mathrm{MM}}(r)$ [solid (*blue*) curves]. The abscissa for the simulated functions are scaled by 1.98/2.09 to reflect the relative positions of the principal peak in the simulated and measured $S_{\mathrm{NN}}(k)$ partial structure factors

large-r oscillations that extend to distances of several nanometres, well beyond the regime associated with the FSDP, with a common periodicity given by $2\pi/k_{\rm PP}$ and a common decay length that is related to $2\pi/\Delta k_{\rm PP}$ where $\Delta k_{\rm PP}$ is the full-width at half-maximum of a principal peak. The number of correlated ions is therefore large e.g. 4060 for a sphere of radius 30 Å in glassy $ZnCl_2$ where $\rho = 0.0359$ Å^{-3} [16]. The character of this extended range ordering is captured by the PIM with $\alpha_{\rm X} = 20$ au as indicated in Fig. 1.2d by the in-phase oscillations in the $g_{\alpha\beta}(r)$ functions at large r-values, and by the $rh_{IJ}(r)$ functions illustrated in Fig. 1.3. A PIM therefore reproduces all of the main features in the structure of $ZnCl_2$ that are observed by experiment.

1.3.1 Simple Theory for Extended Range Ordering

The character of the extended range ordering in network glass-forming materials such as $ZnCl_2$ can be addressed by using simple theory. Let the pair-potential describing the interactions between two ions labelled by i and j separated by a distance r be represented by a RIM given by the expression [66]

$$\phi_{ij}(r) = \phi_{ij}^{\rm sr}(r) + \frac{Z_i Z_j e^2}{\epsilon r} - \frac{A_{ij}}{r^6} \tag{1.12}$$

where $Z_i e$ is the charge on the ith ion, e is the elementary charge, $\varepsilon \equiv 4\pi\varepsilon_r\varepsilon_0$, ε_r is the dimensionless relative dielectric constant of the medium in which the ions are embedded, and ε_0 is the vacuum permittivity. In this equation, $\phi_{ij}^{\rm sr}(r)$ describes the short-ranged repulsive interactions, $\phi_{ij}^{\rm Coul}(r) \propto r^{-1}$ describes the Coulomb interactions, and $\phi_{ij}^{\rm disp}(r) = -A_{ij}r^{-6}$ describes the dispersion interactions where the parameter A_{ij} ($\geq$0) depends on the ion polarisability [67].

For this RIM, a simple power-law dependence for the ultimate decay of the pair correlation functions is expected i.e. $rh_{\rm NN}(r) \to r^{-5}$, $rh_{\rm CC}(r) \to r^{-9}$ and $rh_{\rm NC}(r) \to r^{-7}$ [50, 68]. However, if the dispersion terms are absent in (1.12), then a pole analysis of the k-space solutions to the Ornstein-Zernike equations following the method of Evans and co-workers [69, 70] leads, in the case when the system density is sufficiently high, to the following expressions for the asymptotic decay of the partial pair-correlation functions [50]

$$rh_{\rm NN}(r) \to 2|\mathscr{A}_{\rm NN}|\exp(-a_0 r)\cos(a_1 r - \theta_{\rm NN}), \tag{1.13}$$

$$rh_{\rm CC}(r) \to 2c_{\rm M}c_{\rm X}|\mathscr{A}_{\rm CC}|\exp(-a_0 r)\cos(a_1 r - \theta_{\rm CC}), \tag{1.14}$$

$$rh_{\rm NC}(r) \to 2|\mathscr{A}_{\rm NC}|\exp(-a_0 r)\cos(a_1 r - \theta_{\rm NC}). \tag{1.15}$$

The $rh_{IJ}(r)$ are therefore exponentially damped oscillatory functions with a common decay length given by a_0^{-1} and a common wavelength for the oscillations given by

$2\pi/a_1$. The $\mathscr{A}_{IJ}$ are complex numbers with amplitudes related by $|\mathscr{A}_{\rm NN}||\mathscr{A}_{\rm CC}| = |\mathscr{A}_{\rm NC}|^2$ and the phases are related by $\theta_{\rm NN} + \theta_{\rm CC} = 2\theta_{\rm NC}$. Equations (1.13)–(1.15) also hold for binary mixtures of hard-spheres having different diameters, i.e. when both the Coulomb and dispersion terms are absent from (1.12), where the common wavelength of oscillation is set by one or other of the hard sphere sizes depending on the thermodynamic conditions [71]. The effect on (1.13)–(1.15) of introducing anion polarisability has yet to be fully explored.

1.3.2 Relative Fragility of Tetrahedral Glass-Forming MX_2 Liquids

A systematic variation of the anion polarisability $\alpha_{\rm X}$ within a PIM has been used to investigate the relative "fragility" of network glass-forming MX_2 liquids in which the predominant structural motifs are MX_4 tetrahedra [61]. The fragility is a measure of the rate at which the dynamical properties of a liquid change on approaching the glass transition temperature T_g and can be quantified in terms of a fragility index $m = {\rm d}\log_{10}\eta/{\rm d}\left(T_g/T\right)|_{T=T_g}$ where η is the liquid viscosity and T is the absolute temperature [72, 73]. Figure 1.4a shows the measured relation between

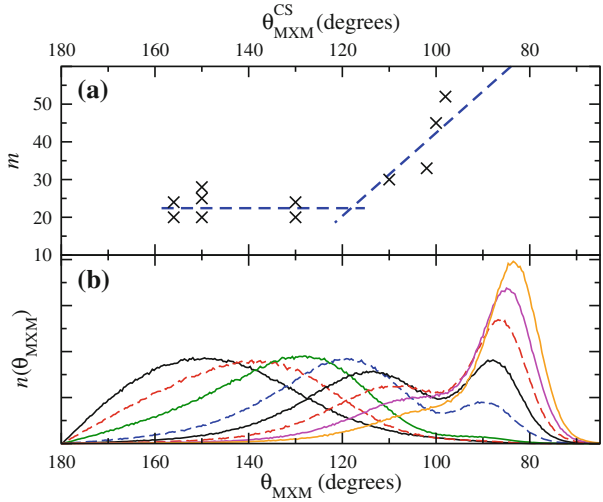

Fig. 1.4 **a** The dependence of the measured fragility index m on the M–X–M bond angle for corner-sharing tetrahedra $\theta^{\rm CS}_{\rm MXM}$ for a series of MX_2 network glass-forming materials. The measured $\theta^{\rm CS}_{\rm MXM}$ values correspond, from left to right, to BeF_2 [77], SiO_2 [78], GeO_2 [78], $ZnCl_2$ [77], GeS_2 [79], $ZnBr_2$ (estimated) and $GeSe_2$ [59]. The fragility values are taken from [73–76]. **b** The M–X–M bond angle distribution $n(\theta_{\rm MXM})$ as calculated using a polarisable ion model (PIM) where the curves, appearing from left to right, correspond to anion polarisability $\alpha_{\rm X}$ values of 0, 5, 10, 15, 17.5, 20, 22.5 and 25 au, respectively. The figure is taken from Wilson and Salmon [61]